Preprints.org

Review

Physicochemical Characterization of a Nano-Hydroxyapatite/β-Tricalcium Phosphate (n-HA/β-TCP) and Type 1 Collagen Composite: An *In Vitro* Study

Igor da silva Brum [*], Carlos Nelson Elias , Bianca Torres Ciambarella ,
Guilherme Aparecido Monteiro Duque da Fonseca , Lucio Frigo , Marco Antonio Carvalho ,
Jorge José de Carvalho

Review

Physicochemical Characterization of a Nano-Hydroxyapatite/β-Tricalcium Phosphate (n-HA/β-TCP) and Type 1 Collagen Composite: An *In Vitro* Study

Igor da Silva Brum [1],*, Carlos Nelson Elias [2], Bianca Torres Ciambarella [3], Guilherme Aparecido Monteiro Duque da Fonseca [4], Lucio Frigo [4], Marco Antônio Alencar de Carvalho [1] and Jorge José de Carvalho [3]

[1] Faculty of Dentistry, State University of Rio de Janeiro, Rio de Janeiro, Brazil.
[2] Materials Science Department, IME Military Engineering Institute, Rio de Janeiro, Brazil.
[3] Department of Histology and Embryology, State University of Rio de Janeiro, Rio de Janeiro, Rio de Jameiro, Brazil
[3] Department of Histology and Embryology, State University of Rio de Janeiro, Rio de Janeiro, Brazil.
[4] Basic Sciences Department, APCD School of Dentistry, São Paulo, Brazil.
* Correspondence: igor_brum1@hotmail.com

Abstract: Materials science has contributed to developing new nano-biomaterials for specific applications in several areas. The present work aims to characterize the physicochemical properties of a composite nanobiomaterial in the form of blocks for application in bone regeneration. The scaffold had block shapes and was a mixture of nano-hydroxyapatite, β-Tricalcium phosphate, and type I collagen of bovine origin. The biomaterial was characterized by scanning electron microscopy (SEM), Transmission Electron Microscopy (TEM), microanalysis, and X-ray diffractometry (XRD). In the SEM and TEM analyses, it was possible to identify the layers of the materials and, with microanalysis, quantify the chemical composition. The XRD spectra showed the presence of nano-hydroxyapatite and nano-ß-TCP. The results showed that the composite does not contain contamination from manufacturing procedures. It can be concluded that the n-HA/β-TCP and type 1 collagen composite is free of manufacturing contaminants and can be suited for clinical testing.

Keywords: nano-hydroxyapatite; ß-TCP; bone; nano-biomaterial; collagen

Introduction

Mixtures of nano-hydroxyapatite with collagen fibers are used to design materials for bone regeneration procedures [1]. The biocompatibilities of collagen fiber and nano-hydroxyapatite promote ideal conditions to create an efficient biomaterial for bone formation process [2].

The physicochemical characteristics of nano-hydroxyapatite (n-HA) prove to be extremely efficient in the bone remodeling process. When compared to micro-hydroxyapatite, the percentage of newly formed matrix and blood vessel proliferation are statistically higher for the n-HA groups, [3].

Type 1 collagen from bovine or other sources, such as porcine pericardium, is widely used as a hemostatic barrier or protective barrier in cases of guided bone regeneration. However, its association with materials that serve as pillar for bone remodeling surgery, such as hydroxyapatite and nano-hydroxyapatite, is being widely developed because the combination of both promotes material stability at the time of surgery and post-surgery [4].

Transmission electron microscopy (TEM) is an excellent tool for determining the collagen bundles present in materials used in guided bone regeneration. Collagen fibrils are very characteristic and the more organized they are, the more organic the sample will be and the better its biocompatibility [5].

Characterization methods, such as scanning electron microscopy (SEM), are necessary to develop new biomaterials. These methods provide high-resolution images to identify the biomaterials in the samples [6].

Semiquantitative chemical analysis using a microprobe coupled to the SEM helps determine the semiquantitative percentages of the chemical elements present in the sample analysis. This technique is suited to identify the possible contaminants from manufacturing procedures that potentially can spoil the material's performance [7].

X-ray diffraction can identify the crystalline phases and chemical elements present in the material. The Rietveld technique quantifies each phase and calculates the chemical percentages of the material [8].

Currently, in the science of biomaterials, the diversity of technical analyses to make it easier and improve the development of biomaterials accelerates the emergence of new potential products. Combining several materials to form a single product becomes a very interesting strategy to improve the final product in several areas, including bone formation [9].

The objective of the present work was to characterize the morphology, identify the crystalline phases, and determine the chemical composition of a composite obtained by combining of nano-hydroxyapatite/β-Tricalcium phosphate and type 1 collagen for use as a biomaterial.

Materials and Methods

The analyzed material, named Blue Bone Block®, was synthetized by an inorganic reaction of two different salts, calcium nitrate and dibasic ammonium phosphate in a very controlled condition keeping the perfect mass balance and the necessary stoichiometry of the reaction, 10:6 Calcium/Phosphorus. The alloplastic biomaterial mixture was synthesized and named Blue Bone® at the facilities of Regener Biomaterials Co (Curitiba, Brazil). The biomaterial had nanometric particles of hydroxyapatite and ß-TCP morphologies.

The collagen type 1 were prepared at Regener® Biomaterials facilities by performing 3 simple steps: cleaning the raw material using two chemical baths, sodium hydroxide and acetone for fat removal; extracting the type 1 collagen using acetic acid from the cleaned bovine tendons; and purifying the extracted material by lyophilization process. The collagen type 1 had an expected reabsorption time of up to 30 days.

The chemical composition of the composite was determined using semi-quantitative chemical analysis with a microprobe coupled to the SEM and TEM.

Scanning Electron Microscopy and Transmission Electron Microscopy

Gold-coated collagen type 1 surfaces were analyzed using a Field Emission GUN Quanta 250 FEG (FEI Company, Oregon, USA). A 5000 magnification was used to investigate the homogeneity, a 15,000 magnification to observe cell clusters, and a 20,000 magnification to identify specific cell types. For the SEM analysis, the fixation procedure started with osmium tetroxide and potassium ferrocyanide (1.0 wt%, 0.8 wt%, respectively) with a cacodylate buffer (0.1 M, pH 7.4) incubation for 1 h in the dark, followed by three sodium cacodylate buffer rinses in distilled water (0.2 M, pH 7.4) for 1 h. This was followed by sequential ethanol grades (25–100 vol%) rinse for specimen dehydration. The slices were immersed in hexamethyl disilazane for 10 min before placing in an evaporation chamber for drying. Specimen mount on aluminum stubs was achieved using colloidal silver adhesive (Electron Microscopy Sciences, Peabody, MA, USA). The specimens were coated with gold film by sputtering (Cool Sputter Coater—SCD 005, Bal-Tec, Berlin, Germany).

The results of SEM analysis were complemented with roughness measurements using a Zygo NewView 7100 optical roughness meter (Zygo Corporation, Connecticut, United States). The implants' roughness parameters Ra, Rsk, Rms, Rku, PV, Rpk, Rk, and R3z were obtained. The analyzed regions presented homogeneous roughness with similar values for all regions.

Thin collagenous type 1 sections were analyzed using a JEOL JEM-1011 transmission electron microscope (JEOL, Ltd., Akishima, Tokyo, Japan), operatin at 60 kV. Digital micrographs were

captured using an ORIUS CCD digital camera (Gatan, Inc., Pleasanton, CA, USA) at 8000×, 10,000× and 25,000× magnification.

The preparation of the samples for TEM analysis was the following: fixation in 2.5 wt% glutaraldehyde diluted in 0.1 M cacodylate buffer solution (overnight). Washing in 3 baths in cacodylate buffer solution (0.1 M), for 15 min each bath. Dehydration in 30 vol% acetone bath (15 min), 50 vol% acetone, 70 vol% acetone (15 min), 90 vol% acetone (15 min), 100 vol% acetone (15 min), and 100 vol% acetone (15 min) Infiltration in acetone + epon mixture (2:1) for 2 h; acetone + epon (1:1) for 2 h; acetone + epon mixture (1:2) for 2 h, infiltration in pure Epon (overnight) Inclusion in Epon and polymerization between 48 and 72 h at 60 °C. Plate cuts with a thickness of 1 micrometer and staining with toluidine blue. Cutting with ultramicrotome to obtain 70 nm slides, which were collected on 300 mesh copper grids. Contrasting of the slides with uranyl acetate (for 20–30 min); and TEM observation.

The X-Ray Diffraction (XRD)

The biomaterial was characterized by X-ray diffraction (XRD), porosimetry, and pycnometer tests. The morphology of the samples was characterized using a scanning electron microscopy (SEM) Field Emission Gun (Quanta FEG 250; Hillsboro, Oregon 97124 - USA).

The X-ray diffraction (XRD) was performed using a Panalytical (Almelo, Netherlands) Empyrean diffractometer, with Cu-Kα radiation, 2θ range of 20–80°, a step width of 0.02°, and an exposure time of 5 s.

The diffraction peaks were identified by comparing them with standard ICDD (International Centre for Diffraction Data) diffraction files and COD-Jan2012 (Crystallography Open Database) PDF2-2004 databases. The Rietveld method was employed to quantify the phases and analyze the crystal structures.

Rietveld analysis of XRD data was used to identify and quantify the percentages of the phases. The X-ray diffractograms were recorded on a Siemens diffractor (Bruker AXS; Durham—UK), model D-5000 (θ-θ), equipped with a graphite curved monochromator, secondary beam and Cu tube. The quantitative analysis of the phases was determined by the mathematical refinement method proposed by Rietveld.

The Rietveld Method involves adjusting the theoretical diffraction peaks calculated from crystallographic information to the experimentally measured diffraction pattern. The criterion for this adjustment is to minimize the sum of the squares of the differences.

Results

The SEM photomicrographs showed different gray shades material bordered by a light clear region. Different regions were aleatory selected for higher magnification and semiquantitative chemical analysis. (Figures 1–3)
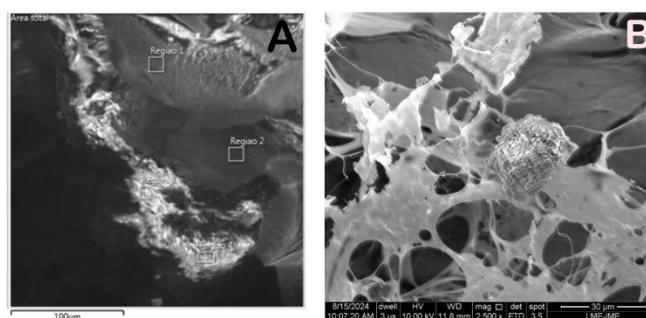

Figure 1. - Micrograph of the sample indicating the regions of chemical analysis in the square boxes (A), and the collagen type I membrane associated with nano-hydroxyapatite/β-tricalcium phosphate. The round particle is a nano-hydroxyapatite/β-tricalcium phosphate (B).

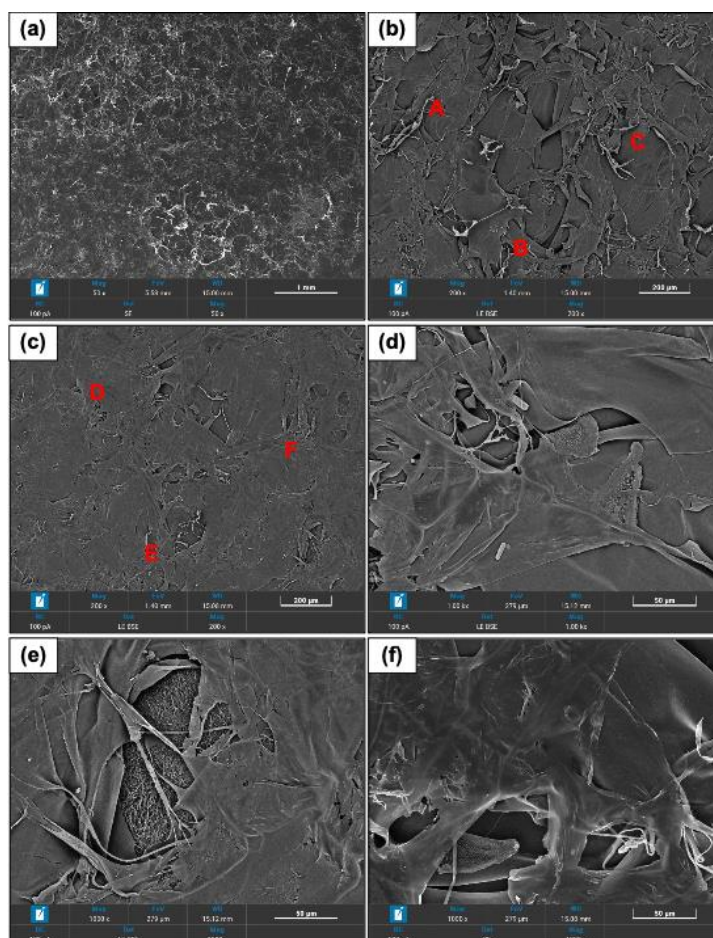The collagen fibrils can be identified as bundles of different thickness and diverse directions (Figure 2a to 2f)

Figure 2. a to 2f - Photomicrographs detailing the points where the semiquantitative chemical analyses were carried out. Figure a (50x); Figures b, c (220x) and Figures d, e, f (1000x) magnification.

The SEM analyzed images showed sheets and plates of collagen in diverse plans of orientations and a highly angulous and porous surfaces of the calcium phosphate granules (Figure 3a, 3b)
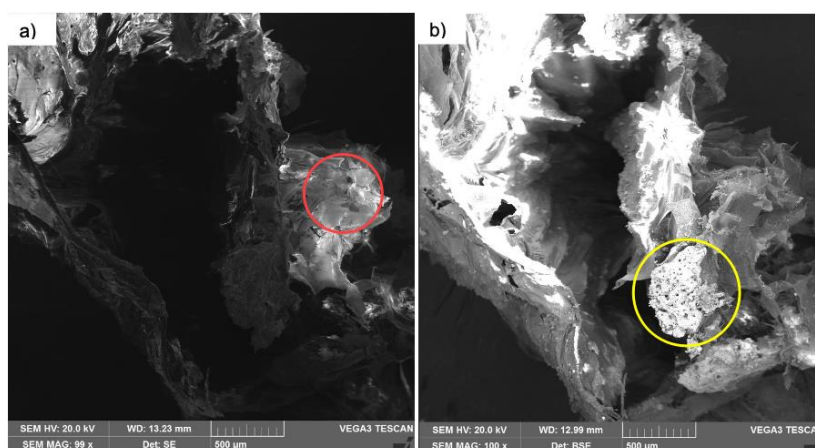

Figure 3. – The SEM photomicrographs of the surface morphology of the analyzed biomaterial. (a) Image obtained with secondary electrons (b) image obtained with backscattered electrons. The area of collagen fibers stands out in the red circle, and the calcium phosphate granule is highlighted in the yellow circle. Figure A (99x) and Figure B (100x) magnification.

Transmission Electron Microscopy (TEM)

Transmission electron microscopy showed the type 1 collagen fibers, which are organically arranged in straight bundles. It was also possible to see that there was no external agent in the type 1 collagen, indicating the purity of the sample. (Figure 4A, 4B)
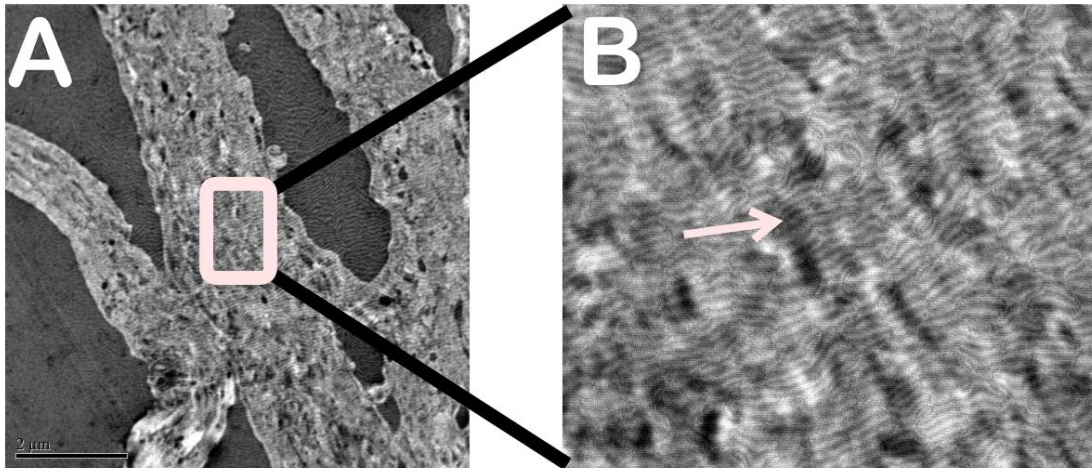

Figure 4. The TEM photomicrograph showed a well-organized type 1 collagen bundles (A) (800x magnification), that is characteristic of this model of bovine type 1 collagen fibrillar pattern (B) (12000x magnification).

Microanalysis of Calcium Phosphate

In the microanalysis of the sample containing calcium phosphate, it was possible to identify the chemical elements forming the n-HA/β-TCP and type 1 collagen composite. (Figure 5a to 5e)
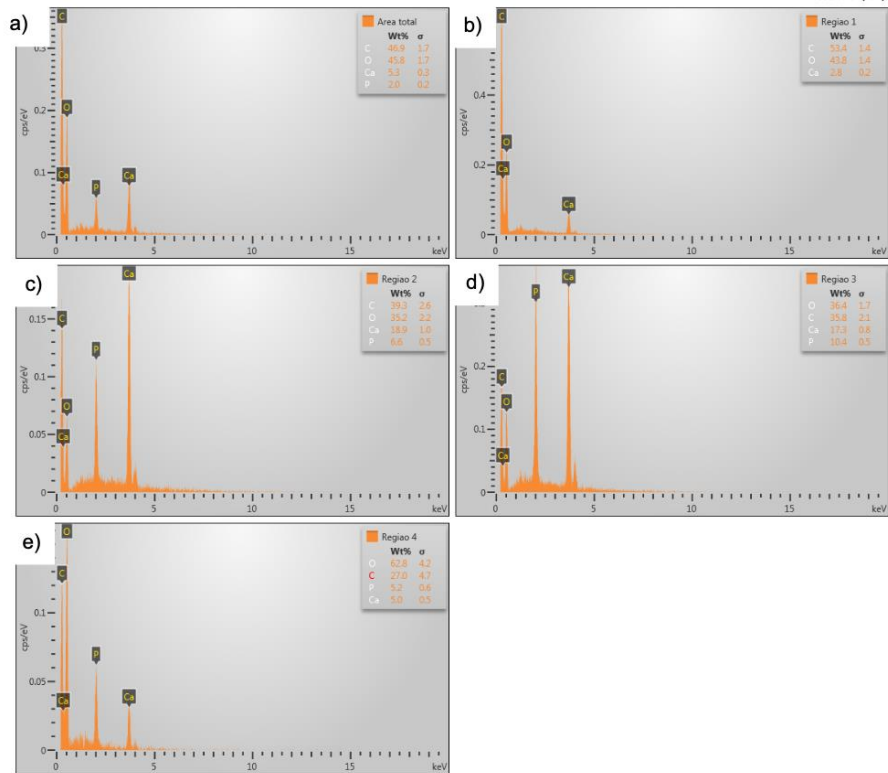

Figure 5. a to 5e - Spectrum of calcium phosphate microanalysis with magnification. Regions analyzed with 1000x magnification.

The chemical percentages of type 1 collagen fibers were recorded, and no impurities were identified. The Figure 6 shows images of the mapping of carbon, nitrogen, and oxygen distribution on the samples' surfaces.
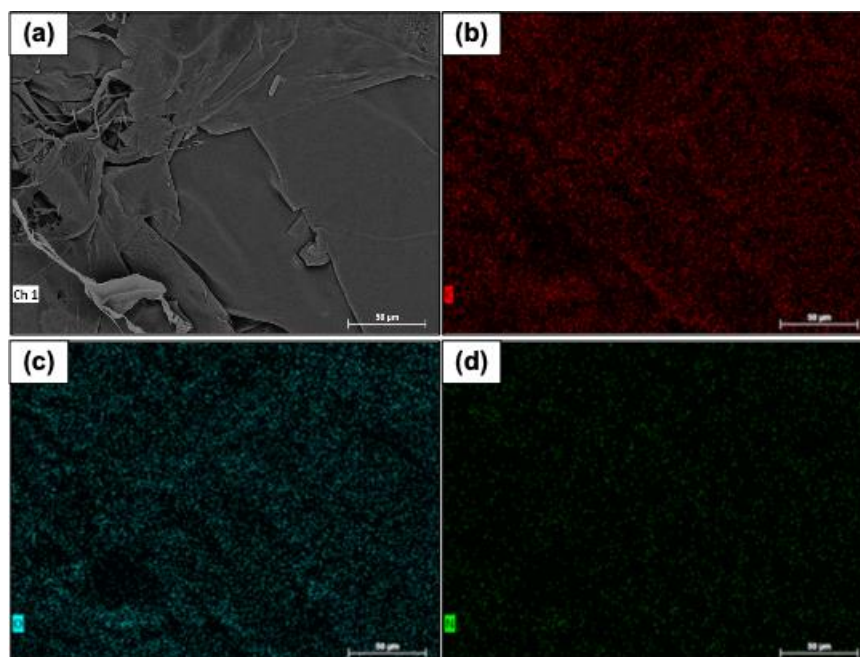

Figure 6. - Mapping of the distribution of chemical elements on the surface of one of the analyzed samples. (a) Mapped area, (b) Carbon (C), (c) Oxygen (O), and (d) Nitrogen (N).

Roughness

Figure 7 shows the image collagenous type 1 surface morphology obtained by interferometry during roughness measurements. The surface was homogeneous. The roughness surface Ra 12.9 µm, Rms 13.1 µm, and Rku 1.1 µm.
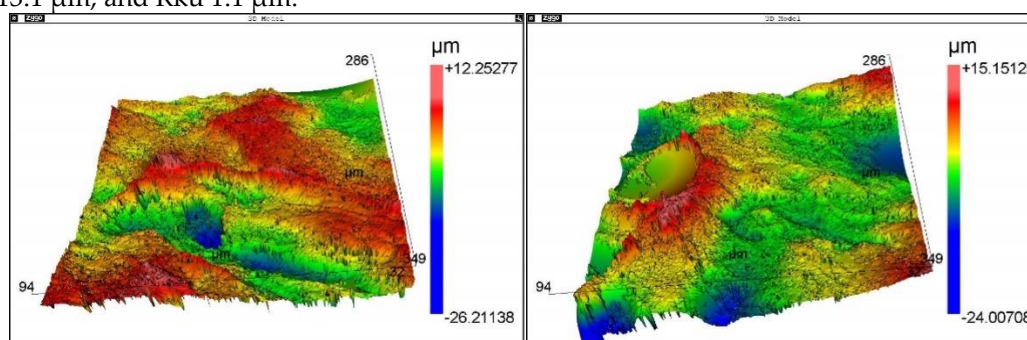

Figure 7. - collagenous type 1 surface morphology. Images obtained by interferometry.

The X-Ray Diffraction (XRD)

Figure 8 shows the diffraction spectra and peaks of the crystalline phases. The peaks of the diffractograms were identified based on information from the database using the Diffrac software. EVE. V4.22.
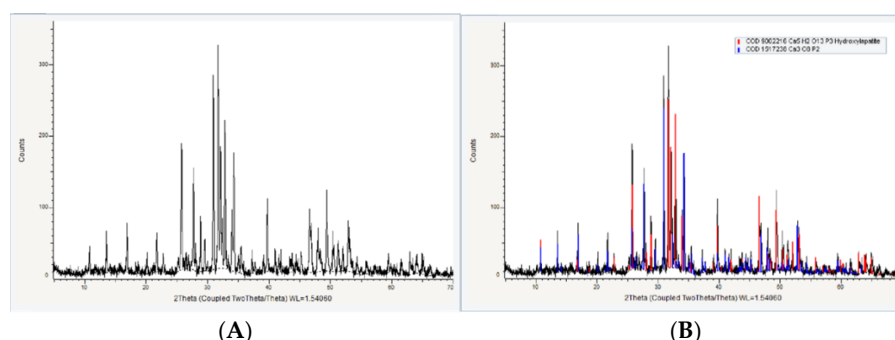
(A)   **(B)**

Figure 8. In the diffractogram of the sample (A) the peaks of the phases characterize only nano-hydroxyapatite while in the diffractogram (B) the peaks of the phases characterize nano-hydroxyapatite (in red) and nano-ß-TCP (in blue).

Discussion

The herein morphological and chemical biomaterial analysis indicates that nano-hydroxyapatite/β-Tricalcium phosphate (n-HA/β-TCP) and type 1 collagen composite is perfectly suitable for further *in vivo* testing.

The development of new graft biomaterials is an excellent alternative to improve the performance of the regenerative properties for patient treatments and adding other types of components to hydroxyapatite has been proven to do so.

Literature data showed that adding chitosan to nano-hydroxyapatite improved osteogenesis and reduced bacterial adhesion [10].

The collagen molecule contributes to key aspects of bone regeneration, such as: cell migration, attachment, migration, cell division and differentiation. Therefore, collagen participates in osteinduction and osteoconduction in bone healing. In addition, collagen is the main scaffold that sustain mineralization in human body, notably in intrafibrillar mineralization pattern [11,12].

Previous work showed that the mixture of hydroxyapatite with collagen had characteristics such as microstructure, absorption kinetics, and mechanical properties suitable as bone substitutes [11]. The results of the present work corroborate those cited in the literature [13–18]. Figure 3 shows the interaction between calcium phosphate and collagen.

A study using rabbits confirmed through several tests, including microanalysis, that the calcium concentration in the material can form different types of hydroxyapatites [19]. In the tests carried out in the present work, it was possible to verify that the percentages of calcium and other chemical elements were similar to those of hydroxyapatite. Figure 3b shows n-HA granules.

The identification of material phases is mainly determined by XRD testing [20–22]. Data from the literature showed that the percentage of nano-hydroxyapatite was similar to that of dentin. The nano-hydroxyapatite induced more collagen cross-links, increased the rate of organic matrix, and promoted better mineralization [23].

The association of nano-hydroxyapatite with collagen was analyzed in tests, and the results were compared with materials containing only hydroxyapatite. The results showed that the structure and performance can be improved by mixing appropriate percentages of collagen and hydroxyapatite [24].

In fact, when nano-hydroxiapatite is mixed with n-HA, the cell viability, cell integration and differentiation processes were improved [25].

Moreover, it was demonstrated that n-HA and collagen scaffolds acted synergistically in osteoconduction process and that bone morphogenetic protein-7 (BMP7) and (BMP2) participated in the process [26].

The results obtained in the present work extended the previous works. It should be noted that the percentages of nano-hydroxyapatite and collagen influence the biomaterial's performance in bone repair.

Conclusion

Based on the results obtained in the present work, it can be concluded that the analyzed nano-biomaterial composed of nano-hydroxyapatite/β-Tricalcium phosphate (n-HA/β-TCP) and type 1 collagen composite does not contain manufacturing processing impurities and is suitable for *in vivo* assays.

References

1. Yu L, Wei M. Biomineralization of Collagen-Based Materials for Hard Tissue Repair. Int J Mol Sci. 2021 Jan 19;22(2):944. doi: 10.3390/ijms22020944. PMID: 33477897; PMCID: PMC7833386.

2. Lazarevic M, Petrovic S, Pierfelice TV, Ignjatovic N, Piattelli A, Vlajic Tovilovic T, Radunovic M. Antimicrobial and Osteogenic Effects of Collagen Membrane Decorated with Chitosan-Nano-Hydroxyapatite. Biomolecules. 2023 Mar 23;13(4):579. doi: 10.3390/biom13040579. PMID: 37189328; PMCID: PMC10135971.

3. Min KH, Kim DH, Kim KH, Seo JH, Pack SP. Biomimetic Scaffolds of Calcium-Based Materials for Bone Regeneration. Biomimetics (Basel). 2024 Aug 24;9(9):511. doi: 10.3390/biomimetics9090511. PMID: 39329533; PMCID: PMC11430767.

4. Carolina DN, Satari MH, Priosoeryanto BP, Susanto A, Sukotjo C, Kartasasmita RE. Synthesis and Structural Characterization of Four Different Concentrations of Ant Nest (*Myrmecodia pendens*) Collagen Membranes with Potential for Medical Applications. Clin Cosmet Investig Dent. 2024 May 27;16:179-189. doi: 10.2147/CCIDE.S446586. PMID: 38827118; PMCID: PMC11141740.

5. Tay FR, Carvalho RM, Yiu CK, King NM, Zhang Y, Agee K, Bouillaguet S, Pashley DH. Mechanical disruption of dentin collagen fibrils during resin-dentin bond testing. J Adhes Dent. 2000 Autumn;2(3):175-92. PMID: 11317391.

6. Hu C, Zilm M, Wei M. Fabrication of intrafibrillar and extrafibrillar mineralized collagen/apatite scaffolds with a hierarchical structure. J Biomed Mater Res A. 2016 May;104(5):1153-61. doi: 10.1002/jbm.a.35649. Epub 2016 Feb 2. PMID: 26748775.

7. da Silva Brum I, de Carvalho JJ, da Silva Pires JL, de Carvalho MAA, Dos Santos LBF, Elias CN. Nanosized hydroxyapatite and β-tricalcium phosphate composite: Physico-chemical, cytotoxicity, morphological properties and in vivo trial. Sci Rep. 2019 Dec 20;9(1):19602. doi: 10.1038/s41598-019-56124-4. PMID: 31863078; PMCID: PMC6925105.

8. Truite CVR, Noronha JNG, Prado GC, Santos LN, Palácios RS, do Nascimento A, Volnistem EA, da Silva Crozatti TT, Francisco CP, Sato F, Weinand WR, Hernandes L, Matioli G. Bioperformance Studies of Biphasic Calcium Phosphate Scaffolds Extracted from Fish Bones Impregnated with Free Curcumin and Complexed with β-Cyclodextrin in Bone Regeneration. Biomolecules. 2022 Feb 28;12(3):383. doi: 10.3390/biom12030383. PMID: 35327575; PMCID: PMC8946016.

9. Zhu X, Bai H, Liu H, Wang Z, Wang Y, Zhang J, Liu J, Wang H, Wang J. A variable mineralization time and solution concentration intervene in the microstructure of biomimetic mineralized collagen and potential osteogenic microenvironment. Front Bioeng Biotechnol. 2023 Dec 6;11:1267912. doi: 10.3389/fbioe.2023.1267912. PMID: 38125304; PMCID: PMC10731298.

10.   Lazarevic M, Petrovic S, Pierfelice TV, Ignjatovic N, Piattelli A, Vlajic Tovilovic T, Radunovic M. Antimicrobial and Osteogenic Effects of Collagen Membrane Decorated with Chitosan-Nano-Hydroxyapatite. Biomolecules. 2023 Mar 23;13(4):579. doi: 10.3390/biom13040579. PMID: 37189328; PMCID: PMC10135971.

11.   Kavitha Sri A, Arthi C, Neya NR, Hikku GS. Nano-hydroxyapatite/collagen composite as scaffold material for bone regeneration. Biomed Mater. 2023 Apr 14;18(3). doi: 10.1088/1748-605X/acc99e. PMID: 37001544.

12.   Selvaraj V, Sekaran S, Dhanasekaran A, Warrier S. Type 1 collagen: Synthesis, structure and key functions in bone mineralization. Differentiation. 2024 Mar-Apr;136:100757. doi: 10.1016/j.diff.2024.100757. Epub 2024 Feb 28. PMID: 38437764.

13.   da Silva Brum I, Elias CN, Nascimento ALR, de Andrade CBV, de Biasi RS, de Carvalho JJ. Ultrastructural and Physicochemical Characterization of a Non-Crosslinked Type 1 Bovine Derived Collagen Membrane. Polymers (Basel). 2021 Nov 26;13(23):4135. doi: 10.3390/polym13234135. PMID: 34883638; PMCID: PMC8659459.

14.   da Silva Brum I, Frigo L, Goncalo Pinto Dos Santos P, Nelson Elias C, da Fonseca GAMD, Jose de Carvalho J. Performance of Nano-Hydroxyapatite/Beta-Tricalcium Phosphate and Xenogenic Hydroxyapatite on Bone Regeneration in Rat Calvarial Defects: Histomorphometric, Immunohistochemical and Ultrastructural Analysis. Int J Nanomedicine. 2021 May 18;16:3473-3485. doi: 10.2147/IJN.S301470. PMID: 34040373; PMCID: PMC8140889.

15.   da Silva Brum I, Frigo L, Lana Devita R, da Silva Pires JL, Hugo Vieira de Oliveira V, Rosa Nascimento AL, de Carvalho JJ. Histomorphometric, Immunohistochemical, Ultrastructural Characterization of a Nano-Hydroxyapatite/Beta-Tricalcium Phosphate Composite and a Bone Xenograft in Sub-Critical Size Bone Defect in Rat Calvaria. Materials (Basel). 2020 Oct 15;13(20):4598. doi: 10.3390/ma13204598. PMID: 33076561; PMCID: PMC7602735.

16.   Ten Huisen KS, Martin RI, Klimkiewicz M, Brown PW. Formation and properties of a synthetic bone composite: hydroxyapatite-collagen. J Biomed Mater Res. 1995 Jul;29(7):803-10. doi: 10.1002/jbm.820290704. PMID: 7593018.

17.   Khan SR, Rodriguez DE, Gower LB, Monga M. Association of Randall plaque with collagen fibers and membrane vesicles. J Urol. 2012 Mar;187(3):1094-100. doi: 10.1016/j.juro.2011.10.125. Epub 2012 Jan 21. PMID: 22266007; PMCID: PMC3625933.

18.   Ruano R, Jaeger RG, Jaeger MM. Effect of a ceramic and a non-ceramic hydroxyapatite on cell growth and procollagen synthesis of cultured human gingival fibroblasts. J Periodontol. 2000 Apr;71(4):540-5. doi: 10.1902/jop.2000.71.4.540. PMID: 10807115.

19.   Serre CM, Papillard M, Chavassieux P, Boivin G. In vitro induction of a calcifying matrix by biomaterials constituted of collagen and/or hydroxyapatite: an ultrastructural comparison of three types of biomaterials. Biomaterials. 1993;14(2):97-106. doi: 10.1016/0142-9612(93)90217-p. PMID: 8382091.

20.   Ohira T, Ishikawa K. Hydroxyapatite deposition in articular cartilage by intra-articular injections of methylprednisolone. A histological, ultrastructural, and x-ray-microprobe analysis in rabbits. J Bone Joint Surg Am. 1986 Apr;68(4):509-20. PMID: 3007526.

21.   Lei X, Gao J, Xing F, Zhang Y, Ma Y, Zhang G. Comparative evaluation of the physicochemical properties of nano-hydroxyapatite/collagen and natural bone ceramic/collagen scaffolds and their osteogenesis-promoting effect on MC3T3-E1 cells. Regen Biomater. 2019 Dec;6(6):361-371. doi: 10.1093/rb/rbz026. Epub 2019 Oct 5. PMID: 31827888; PMCID: PMC6897342.

22.   El-Fiqi A, Kim JH, Kim HW. Novel bone-mimetic nanohydroxyapatite/collagen porous scaffolds biomimetically mineralized from surface silanized mesoporous nanobioglass/collagen hybrid scaffold: Physicochemical, mechanical and in vivo evaluations. Mater Sci Eng C Mater Biol Appl. 2020 May;110:110660. doi: 10.1016/j.msec.2020.110660. Epub 2020 Jan 11. PMID: 32204088.

23.   Kim SC, Heo SY, Oh GW, Yi M, Jung WK. A 3D-Printed Polycaprolactone/Marine Collagen Scaffold Reinforced with Carbonated Hydroxyapatite from Fish Bones for Bone Regeneration. Mar Drugs. 2022 May 25;20(6):344. doi: 10.3390/md20060344. PMID: 35736147; PMCID: PMC9230561.

24. Epasinghe DJ, Kwan S, Chu D, Lei MM, Burrow MF, Yiu CKY. Synergistic effects of proanthocyanidin, tri-calcium phosphate and fluoride on artificial root caries and dentine collagen. Mater Sci Eng C Mater Biol Appl. 2017 Apr 1;73:293-299. doi: 10.1016/j.msec.2016.11.078. Epub 2016 Nov 22. PMID: 28183611.

25. Enrich-Essvein T, Rodríguez-Navarro AB, Álvarez-Lloret P, Cifuentes-Jiménez C, Bolaños-Carmona MV, González-López S. Proanthocyanidin-functionalized hydroxyapatite nanoparticles as dentin biomodifier. Dent Mater. 2021 Sep;37(9):1437-1445. doi: 10.1016/j.dental.2021.07.002. Epub 2021 Aug 3. PMID: 34353622.

26. Wang YF, Wang CY, Wan P, Wang SG, Wang XM. Comparison of bone regeneration in alveolar bone of dogs on mineralized collagen grafts with two composition ratios of nano-hydroxyapatite and collagen. Regen Biomater. 2016 Mar;3(1):33-40. doi: 10.1093/rb/rbv025. Epub 2015 Dec 31. PMID: 26816654; PMCID: PMC472327